A Printed Wideband MIMO Antenna for Mobile and Portable Communication Devices

Chan H. See[1,2], Elmahdi Elkazmi[2,3], Khalid G. Samarah[2,4], Majid Al Khambashi[2,3], Ammar Ali[2], Raed A. Abd-Alhameed[2(✉)], Neil J. McEwan[5], and Peter S. Excell[6]

[1] School of Engineering, University of Bolton, Deane Road, Lancashire, Bolton, BL3 5AB, UK
[2] School of Electrical Engineering and Computer Science, University of Bradford, Richmond Road, West Yorkshire, Bradford, BD7 1DP, UK
{chsee2,raaabd}@bradford.ac.uk
[3] The Higher Institute of Electronics, Bani Walid, Libya
[4] Mutah University, Al-Karak 61710, Jordon
[5] AlZahra College for Women, Muscat, Oman
[6] School of Computing and Communication Technology, Glyndwr University, Mold Road, Wrexham LL11 2AW, Wales, UK

Abstract. A printed crescent-shaped monopole MIMO antenna is presented for handheld wireless communication devices. The mutual coupling between the two antenna elements can be minimised by implementing a I-shaped common radiator. Both the simulated and measured results agree that the antenna covers the operating frequency band from 1.6 to 2.8 GHz with the return loss and isolation better than 10 dB and 14 dB respectively. To further verifying the MIMO characteristic including far-field, gain, radiation efficiency, channel capacity loss and envelope correlation, the results confirm that the antenna can operate effectively in a rich multipath environment.

Keywords: MIMO · Mutual coupling · Channel capacity loss · Envelope correlation

1 Introduction

The increasing use of smart phones and tablet computers has resulted in substantial teletraffic growth. Clearly, the current capacity and bandwidth of the existing wireless communication systems are insufficient to meet the needs of next generation mobile requirements. In anticipation of this, new high data-rate wireless systems, such as HSPA (3.5G), LTE (4G), WiFi, WiMAX and UWB, have been developed [1–3]. It is expected that future mobile devices will be required to inter-operate seamlessly with all the existing second and third generation mobile standards as well as with these new enhanced standards. To help cater for this unabated demand for high data-rate traffic resulting from ever-growing mobile applications, these existing wireless standards require a multiple-input-multiple-output (MIMO) antenna system.

P. Pillai et al. (Eds.): WiSATS 2015, LNICST 154, pp. 239–248, 2015.
DOI: 10.1007/978-3-319-25479-1_18

It is well known that the use of multiple antennas on both the transmitting and receiving ends of a communication system promises to deliver robust communication links with enhanced data-rate, without increasing the power and spectrum requirement, when operating in a multi-user rich scattering environment [2, 4, 5]. Nevertheless, implementing the MIMO antenna technology in a handheld device remains a challenge for antenna engineers due to the limited space within an existing commercial mobile chassis. MIMO antennas have to satisfy all the performance indicators of a single-element antenna and also require a good port-to-port isolation between the closely placed antenna elements.

Over the last five years, much research effort has been invested in conceiving solutions capable of minimizing the mutual coupling between MIMO antenna elements. These solutions can be classified into three categories, i.e. narrow band [6, 8–17], wideband [18–21] and dual band [22–25]. In the narrow band applications, MIMO antennas were developed to operate with the following wireless standards, LTE 700–800 MHz [6–8], UMTS [9], WLAN 2.4 GHz [10–13], 5.2 GHz [14] and 5.8 GHz [15, 16]. To suppress the mutual coupling between the antenna elements, these antennas have adopted several innovative methods including ferrite [6] or magneto-dielectric substrates [7], the insertion of parasitic elements between the radiators [8, 9], introducing resonators between the antenna elements [10], connecting the elements via a neutralization line [11], etching a series of slits in the ground plane [12], utilizing lumped elements [13] or inductive coils [14], heavily slotting the ground plane [15], placing the antenna elements in an orthogonal formation [16], and adopting varactor diode and lumped elements [17]. These solutions achieve a good port-to-port isolation ranging from 10 dB to 40 dB, and reasonable inter-element distances from 0.03 λ_0 to 0.17 λ_0.

By compromising between the bandwidth, mutual coupling level and inter-element spacing distance of a MIMO antenna, some wideband isolation methods were proposed in [18–21] to enable multiband operation. In [18], it was found that by separating the two antenna elements by 0.25 λ_0, mutual coupling as good as −11 dB can be attained across the frequency band from 1.65 to 2.5 GHz. Other work in [19] demonstrates that by placing the antenna elements orthogonally, the inter-port isolation level can be enhanced to 20 dB with an element spacing of 0.1λ_0, covering an operating band from 1.63 to 2.05 GHz. Moreover, the author in [20] suggests that using inverted L-parasitic monopoles offers a wideband inter-port isolation of better than 14.8 dB from 1.85 to 2.170 GHz. In addition, the work in [21] proposes placing branched neutralization lines between the antenna elements which can suppress the mutual coupling to better than −17 dB over a wide frequency band, from 2.4 to 4.2 GHz.

Apart from narrow band and wideband inter-port isolation methods, some dual band methods have also been introduced in [22–25]. Interestingly, it was noticed that good dual band port-to-port isolation can be realized by using either a modified version of single band methods or combinations of them. In [22], the authors show that inserting both a T-shaped and a dual inverted L-shaped branch in the ground plane can provide a good isolation of 13 dB and 18 dB over the UMTS and WLAN 2.4 GHz bands respectively. Furthermore, to suppress the mutual coupling of two antenna elements in two distinct sub-bands, i.e. WLAN 2.4 GHz and WiMAX 3.5 GHz, the authors in [23] recommend that implementing a T-shaped slot in the ground plane and a folded L-slot in the radiator can effectively reduce mutual coupling to 19.2 dB and 22.8 dB over the

two bands correspondingly. On the other hand, authors in [24] also show that, by carefully adjusting the lengths of proposed parasitic elements, isolation better than 15 dB and 22 dB can be obtained over the two frequency bands, i.e. WLAN 2.4 GHz and 5.8 GHz. However, these methods only offer operation in narrow band wireless standards. To overcome this limitation, a dual wideband MIMO antenna was studied in [25]. In this work, two U-shaped slots were etched in the ground plane to act as a decoupling network. Both the outer and inner slots improve the inter-port isolation to better than 15 dB and 20 dB over the two wide sub-bands, i.e. 1.5–2.8 GHz and 4.7 to 8.5 GHz, respectively.

In summary, it is found that most of these antennas only provide either single or dual narrow band operation [15–17, 22–24], or wideband operation [18–21] but do not fully cover many existing mobile standards, except for the work in [25]. To address this limitation, this paper presents a MIMO/diversity monopole antenna for GSM1800/1900 (1710–1880 MHz, 1850–1990 MHz), UMTS2000 (1920–2170 MHz), LTE2300 (2300–2400 MHz), LTE2600 (2500–2690 MHz), WiFi (2400–2485 MHz) and WiMAX (2500–2690 MHz) applications. By inserting an **I** - shaped metal strip on a defected ground plane which is located underneath the two antenna elements, an inter-port isolation as good as 14 dB can be realized with return loss better than 10 dB across all the operating frequency bands.

2 Antenna Design Concept and Geometry

Figure 1 illustrates the configuration of the proposed MIMO/diversity antenna. It consists of two metallic layers where the top layer has two radiating elements and the bottom layer is a modified defected ground plane. Both layers are printed on a Duroid 5870 substrate material with a thickness of 0.79 mm, dielectric constant (ε_r) of 2.33 and a loss tangent of 0.0012. The single element of the radiator is very similar to the one in [21, 26], except that the ends of the radiator have straight extensions. The crescent-shaped radiator is fed by an 18 x 1 mm microstrip line. This line has lower and upper sections of length 11.25 mm and 6.75 mm respectively. The lower section which lies over the ground plane has a characteristic impedance of 83 Ω and is required for matching to 50 Ω at the input port. The dimensions of the ground plane are 71.5 x 50 mm^2 with a defected area of 26.8 x 12 mm^2 in its top edge, this being used to improve the impedance matching at the input port. The overall dimensions of the proposed antenna are $90 \times 50 \times 0.8$ mm which is suitable for application in a typical handheld device.

The design procedure of this antenna begins with optimizing a single element crescent-shaped radiator on a corner of a 50 x 90 mm ground plane. By manipulating the radii r1 and r2 of the geometry parameters (Fig. 1), the lower and upper resonant frequencies can be adjusted to establish a wide impedance bandwidth [21]. In order to improve the impedance matching for return loss to better than 10 dB over the band, the length of the crescent-shaped radiator's straight extensions (d) was further optimized and a defected area of 26.8×11.25 mm^2 was introduced in the ground plane. Once the targeted performance of a single element antenna was realized, two identical copies of the radiators were symmetrically placed on the two corners of the ground plane. These two radiators are separated by the largest possible distance of 24 mm which is equivalent

to 0.128 λ_0 (where λ_0 is the free space wavelength) at 1.6 GHz (i.e. the lowest working frequency) for the optimal mutual coupling suppression. The final design stage was to insert an **I** -shaped strip on the ground plane of the antenna and to find its geometric parameters for best performance in terms of reflection coefficient and mutual coupling.

Confirming the effectiveness of the **I** -shaped strip, Fig. 2 shows the S-parameters of the proposed antenna with and without the strip. In the $|S_{11}|$ plot, without the strip, the impedance bandwidth covers 1.55 GHz to 2.5 GHz band, thus setting |S11| as better than −10 dB. However, the insertion of the strip results in a wider impedance bandwidth which accommodates the band from 1.6 to 2.8 GHz with two clearly distinct resonant frequencies, i.e. 1.7 GHz and 2.4 GHz. Examining the $|S_{21}|$ curves, the mutual coupling has been improved by −5 dB from −9 to −14 dB over the entire band comparing the cases with and without the **I** -shape. Thus the **I** -shaped structure is acting as an impedance bandwidth enhancement and inter-element decoupling network.

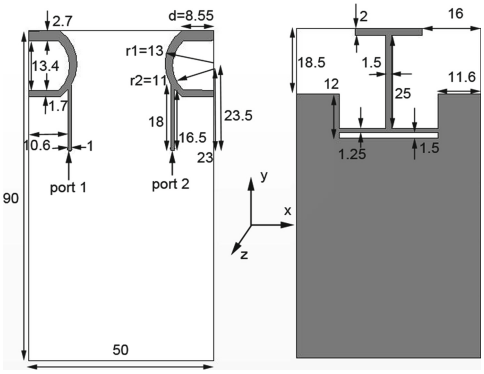

Fig. 1. The geometry of proposed printed planar MIMO antenna

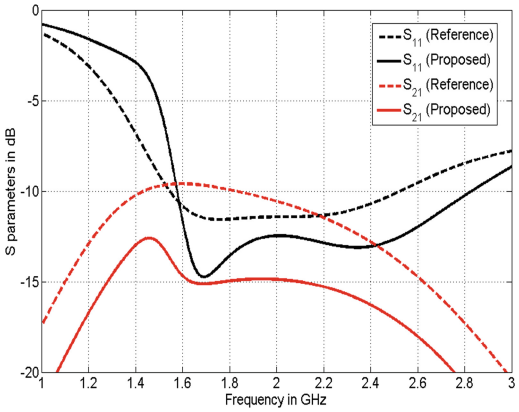

Fig. 2. Simulated S-parameters of the proposed antenna with and without the I-shaped structure.

To further understand the contribution of the **I** - shaped structure to the performance, the surface current distributions of the antenna with and without this structure are also illustrated in Fig. 3. In this study, two frequencies of 1.7 and 2.5 GHz were selected, representing lower and upper points in the desired frequency band. As can be clearly noticed, when port 1 is excited and port 2 is terminated in 50 Ω without the **I** - shaped structure, a strong induced current appears on the port 2 antenna element. This can be attributed to the presence of a near field coupling current and a shared common ground plane current when the two antennas are closely placed. However, when the structure is introduced on the ground plane, it is found that the surface current is trapped on this structure and this attenuates the induced current on the port 2 of the antenna elements. This tends to decouple the currents on the port 2 radiator and hence improves the inter-port isolation between the antenna elements.

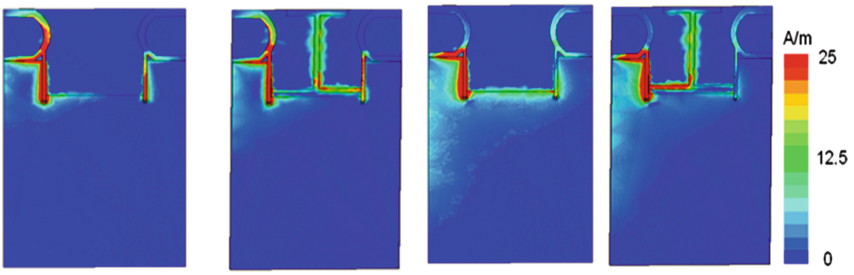

Fig. 3. Contour plot surface current distributions with and without the **I** - shape at (i) 1.7 GHz, and (ii) 2.5 GHz. Port 1 (left) is excited and port 2 (right) is terminated in 50Ω.

3 Results and Discussion

A prototype of the proposed antenna was fabricated as shown in Fig. 4 and tested in order to validate the simulated results. Figure 5 compares the computed and experimental reflection $|S_{11}|$ and mutual coupling $|S_{21}|$ coefficients of the antenna. Observing the $|S_{11}|$ plots, these exhibit an impedance bandwidth of 1.2 GHz, from 1.6 to 2.8 GHz for the criterion of $|S_{11}|$ better than −10 dB, which is equivalent to 54.5 %. This wide bandwidth enables the antenna to meet the requirements of the GSM1800/1900, UMTS2000, LET2300, LT2600, WiFi and WiMAX frequency bands. Further scrutinizing the mutual coupling $|S_{21}|$ curves, it is notable that inter-element mutual coupling is better than −14 dB over the entire operating frequency band. Both simulated and measured results are in satisfactory agreement, and minor discrepancies in these results can be attributed to fabrication tolerances, SMA connector effects and some uncertainty in the electrical properties of the substrate material.

Fig. 4. Practical prototype of the proposed antenna

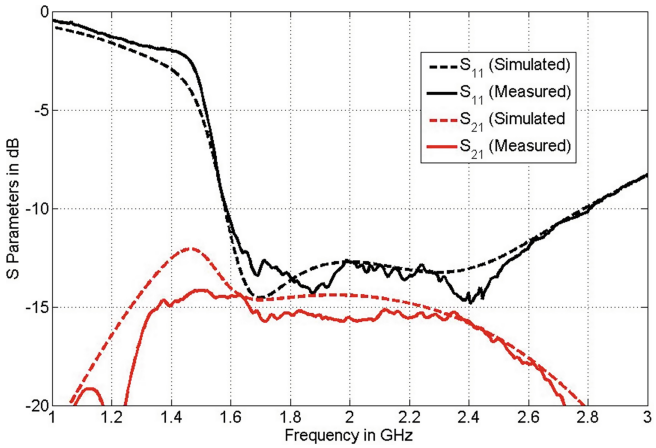

Fig. 5. S parameters of the proposed antenna

To check the MIMO/diversity performance of the proposed antenna, the two key performance indicators, i.e. envelope correlation coefficient (ECC) and channel capacity loss, will be considered. It is well known that ECC can be computed by using 3D far-field data [4, 5] and S-parameters [11, 21, 25] methods, but as the far-field method is very time consuming and involves complex integral calculations of radiation pattern data, the S-parameters method, as described in [11, 21, 25], was adopted. The simulated and measured ECC of the MIMO antenna are presented in Fig. 6(a), showing that computed and experimental results are in good agreement. ECC values for the antenna are less than 0.006 over the targeted operating frequency band. These results are comparable to the published results in [11, 21, 25]. The simplified channel capacity loss of a 2×2 MIMO system can be evaluated by using the following equation, given in [11, 21]:

$$C_{loss} = -\log_2 \det(\psi^R) \tag{1}$$

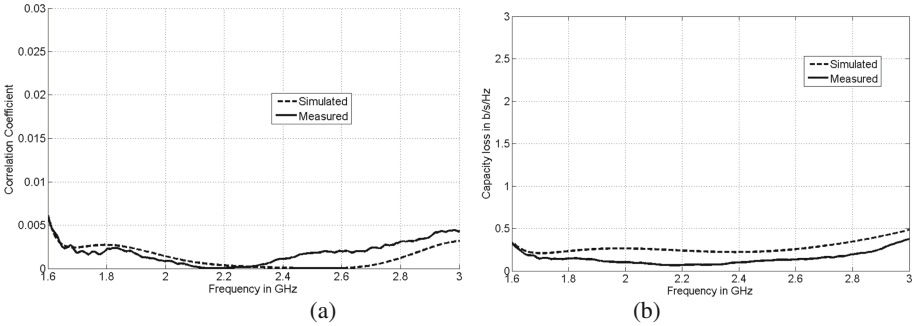

Fig. 6. Simulated and measured MIMO characteristics of the proposed antenna, (a) correlation coefficient, (b) capacity loss

where ψ^R is the receiving antenna correlation matrix: $\psi^R = \begin{bmatrix} \rho_{11} & \rho_{12} \\ \rho_{21} & \rho_{22} \end{bmatrix}$,

with $\rho_{ii} = 1 - \left(|S_{ii}|^2 + |S_{ij}|^2 \right)$, and $\rho_{ij} = - \left(S_{ii}^* S_{ij} + S_{ji}^* S_{jj} \right)$, for i, j = 1 or 2.

Using the above formulas, simulated and measured channel capacity loss of the MIMO antenna can be estimated as less than 0.3 b/s/Hz, which is acceptable for practical MIMO systems [11, 25]. Small discrepancies between the results can be attributed to fabrication errors and feed cable effects.

Figure 7 shows the simulated and measured peak gains of the MIMO antenna over the 1.6 to 2.8 GHz frequency band. Here the peak gain is about 1.7–2.5 dBi and 1.2–2.3 dBi for the computed and experimental results respectively over the band. The worst disagreement between the simulation and measurement is about 0.5 dBi at the lowest operating frequency, i.e. 1.6 GHz. To demonstrate the consistency of the radiation pattern over all designated operating frequency bands, simulated and measured radiation patterns of the proposed antenna are shown in Fig. 8. Since the structure of the antenna element differs substantially from conventional designs, it is difficult to predict its radiation pattern behavior other than by simulation. In the measurements, three pattern cuts (i.e. x-z, y-z and x-y planes) were taken at two representative operating frequencies, i.e. 1.8 and 2.4 GHz. The presented results show that the radiation patterns are consistent at these two frequencies, and the computed and measured radiation patterns are seen to be in acceptable agreement. Some small discrepancies between the simulated and measured results can be attributed to the physical feeding arrangements. It should be highlighted that the cross-polarization ratio of this antenna is acceptable, as the issue of polarization purity is not critical for this antenna's use in portable devices.

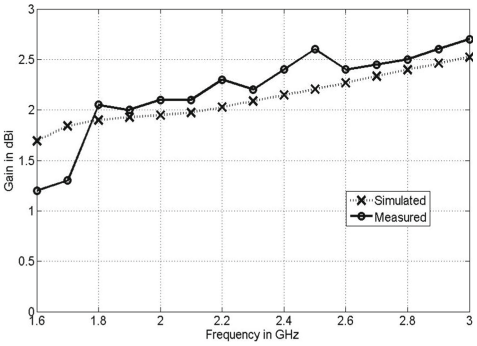

Fig. 7. Measured and simulated peak gains of the proposed antenna.

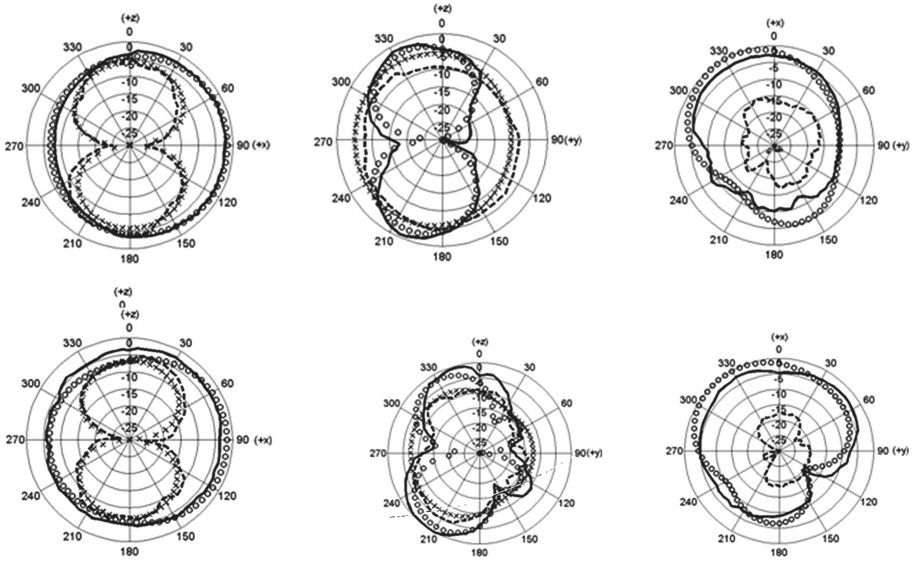

Fig. 8. Simulated and measured normalized radiation patterns of the proposed antenna for three planes (left: x-z plane, centre: y-z plane and right: x-y plane) at (a) 1.8 GHz and (b) 2.4 GHz 'xxxx' simulated cross-polarization 'oooo' simulated co-polarization '------' measured cross-polarization '——' measured co-polarization

4 Conclusion

A broadband printed MIMO monopole antenna which is suitable for commercial mobile/ wireless handheld devices was developed. It offers a wide operating frequency band from 1.6 GHz to 2.8 GHz corresponding to a bandwidth of 1.2 GHz. To achieve a good isolation between the two antenna elements, an **I** - shaped strip was introduced in a defected ground plane to effectively enhance the bandwidth and suppress the mutual

coupling. By implementing this, inter-port isolation as good as 14 dB and return loss better than 10 dB across the designated frequency band was realized. This diversity antenna, with envelope dimensions of 50 x 90 x 0.8 mm^3, exhibits sufficient impedance bandwidth, suitable radiation characteristics, adequate gains, and low correlation coefficient and channel capacity loss for GSM1800/1900, UMTS2000, LTE 2300, LTE2600, WiFi (2.4 GHz) and WiMAX (2.5 GHz) applications.

References

1. Hanzo, L., Haas, L., Imre, S., O'Brien, D., Rupp, M., Gyongyosi, L.: Wireless myths, realities, and futures: from 3G/4G to optical and quantum wireless. Proc. IEEE **100**, 1853–1888 (2012)
2. Hanzo, L., El-Hajjar, M., Alamri, O.: Near-capacity wireless transceivers and cooperative communications in the MIMO era: evolution of standards, waveform design, and future perspectives. Proc. IEEE **99**(8), 1343–1385 (2011)
3. Ying, L.: Antennas in cellular phones for mobile communications. Proc. IEEE **101**, 2286–2296 (2012)
4. Shin, H., Lee, J.H.: Capacity of multiple-antenna fading channels: spatial fading correlation, double scattering, and keyhole. IEEE Trans. Inform. Theory **49**, 2636–2647 (2003)
5. Wallace, J., Jensen, M., Swindlehurst, A., Jeffs, B.: Experimental characterization of the MIMO wireless channel: data acquisition and analysis. IEEE Trans. Wirel. Commun. **2**, 335–343 (2003)
6. Shin, Y.S., Park, S.O.: A monopole antenna with a magneto-dielectric material and its MIMO applications for 700 MHz LTE-band. Microw. Opt. Technol. Lett. **52**, 603–606 (2010)
7. Lee, J., Hong, Y.-K., Bae, S., Abo, G.S., Seong, W.-M., Kim, G.-H.: Miniature long-term evolution (LTE) MIMO ferrite antenna. IEEE Antennas Wirel. Propag. Lett. **10**, 2364–2367 (2011)
8. Sharawi, M.S., Iqbal, S.S., Faouri, Y.S.: An 800 MHz 2 X 1 compact MIMO antenna system for LTE handsets. IEEE Trans. Antennas Propag. **59**, 3128–3131 (2011)
9. Li, Z., Du, Z., Takahashi, M., Saito, K., Ito, K.: Reducing mutual coupling of MIMO antennas with parasitic elements for mobile terminals. IEEE Trans. Antennas Propag. **60**, 473–481 (2012)
10. Minz, L., Garg, R.: Reduction of mutual coupling between closely spaced PIFAs. Electron. Lett. **46**, 392–394 (2010)
11. Su, S.-W., Lee, C.T., Chang, F.-S.: Printed MIMO-antenna system using neutralization-line technique for wireless USB-Dongle applications. IEEE Trans. Antennas Propag. **60**, 456–463 (2012)
12. Li, H., Xiong, J., He, S.: A compact planar MIMO antenna system of four elements with similar radiation characteristic and isolation structure. IEEE Antennas Wirel. Propag. Lett. **8**, 1107–1110 (2009)
13. Chen, S.-C., Wang, Y.-S., Chung, S.-J.: A decoupling technique for increasing the port isolation between two strongly coupled antennas. IEEE Trans. Antennas Propag. **56**, 3650–3658 (2008)
14. Krairiksh, M., Keowsawat, P., Phongcharoenpanich, C.: Two-probe excited circular ring antenna for MIMO application. Prog. Electromagnetics Res. **97**, 417–431 (2009)
15. OuYang, J., Yang, F., Wang, Z.M.: Reducing mutual coupling of closely spaced microstrip MIMO antennas for WLAN application. IEEE Antennas Wirel. Propag. Lett. **10**, 310–313 (2011)

16. Mallahzadeh, A.R., Es'haghi, S., Alipour, A.: Design of an E shaped MIMO antenna using IWO algorithm for wireless application at 5.8 GHz. Prog. Electromagnetics Res. **97**, 417–431 (2009)
17. Tang, X., Mouthaan, K., Coetzee, J.C.: Tunable decoupling and matching network for diversity enhancement of closely spaced antennas. IEEE Antennas Wirel. Propag. Lett. **11**, 268–271 (2012)
18. Zhou, X., Li, R., Jin, G., Tentzeris, M.M.: A compact broadband MIMO antenna for mobile handset applications. Microw. Opt. Technol. Lett. **53**, 2773–2776 (2011)
19. Zhang, S., Zetterberg, P., He, S.: Printed MIMO antenna system of four closely-spaced elements with large bandwidth and high isolation. Electron. Lett. **46**, 1052–1053 (2010)
20. Kang, G., Du, Z., Gong, K.: Compact broadband printed slot-monopole-hybrid diversity antenna for mobile terminal. IEEE Antennas Wirel. Propag. Lett. **10**, 159–162 (2011)
21. See, C.H., Abd-Alhameed, R.A., Abidin, Z.Z., McEwan, N.J., Excell, P.S.: Wideband printed MIMO/Diversity monopole antenna for WiFi/WiMAX applications. IEEE Trans. Antennas Propag. **60**, 2028–2035 (2012)
22. Ding, Y., Du, Z., Gong, K., Feng, Z.: A novel dual-band printed diversity antenna for mobile terminals. IEEE Trans. Antenna Propag. **55**, 2088–2096 (2007)
23. Zhang, S., Lau, B.K., Tan, Y., Ying, Z., He, S.: Mutual coupling reduction of two PIFA with a T-shape slot impedance transformer for MIMO mobile terminals. IEEE Trans. Antennas Propag. **60**, 1521–1531 (2012)
24. Addaci, R., Diallo, A., Luxey, C., Thuc, P.L., Staraj, R.: Dual-Band wlan diversity antenna-system with high port-to-port isolation. IEEE Antennas Wireless Propag. Lett. **11**, 244–247 (2012)
25. Zhou, X., Quan, X., Li, R.: A dual-broadband MIMO antenna system for GSM/UMTS/LTE and WLAN handsets. IEEE Antennas Wirel. Propag. Lett. **11**, 514–551 (2012)
26. See, C.H., Abd-Alhameed, R.A., Zhou, D., Lee, T.H., Excell, P.S.: A crescent-shaped multiband planar monopole antenna for mobile wireless applications. IEEE Antenna Wirel. Propag. Lett. **9**, 152–155 (2010)